HHS Public Access

Author manuscript

Clin Nutr. Author manuscript; available in PMC 2022 June 22.

Published in final edited form as:

Clin Nutr. 2021 April ; 40(4): 2435–2442. doi:10.1016/j.clnu.2020.10.046.

Establishment of normative biometric data for body composition based on computed tomography in a North American cohort

P.J. Navin[a],

M.R. Moynagh[a],

E.J. Atkinson[b],

P. Tirumanisetty[c],

N.K. LeBrasseur[d],

A. Kumar[e],

S. Khosla[f],

N. Takahashi[a,*]

[a]Department of Radiology, Mayo Clinic, Rochester, USA

[b]Department of Health Sciences Research, Mayo Clinic, Rochester, USA

[c]Department of Gastroenterology and Hepatology, Mayo Clinic, Rochester, USA

[d]Department of Physical Medicine and Rehabilitation, Mayo Clinic, Rochester, USA

[e]Department of Gynecological Surgery, Mayo Clinic, Rochester, USA

[f]Department of Endocrinology, Mayo Clinic, Rochester, USA

SUMMARY

Background & aims: Accurate and reproducible biomarkers are required to allow a more personalized approach to patient care. Body composition is one such biomarker affecting outcomes in a range of surgical and oncological conditions. The aim of this study is to determine the age and sex specific distribution of body composition data, based on information gathered from computed tomography (CT).

Methods: This prospective study used healthy subjects from the medical records linkage of the Rochester Epidemiology Project, based in Minnesota, USA. Each patient had a CT scan without intravenous contrast performed between 1999 and 2001. Quantification was performed using previously validated semi-automated in-house developed software for body composition analysis. Subcutaneous adipose tissue area, visceral adipose tissue area, intermuscular adipose tissue area and skeletal muscle area were measured and indexed to subject height. Generalized Additive Models for Location, Scale and Shape were used to assess the location, scale, and shape of each variable across age, stratified by sex. Z-scores specific to sex were assessed for each of the

*Corresponding author. Fax: +5072664743. Takahashi.Naoki@mayo.edu (N. Takahashi).

Conflict of interest

PJ Navin, MR Moynagh, EJ Atkinson, P Tirumanisetty, N Lebrasseur, A Kumar, S Khosla and N Takahashi all declare no conflict of interest.

parameters analyzed. Age-specific z-scores were calculated using the formula: Z = (Index Variable − μ)/σ or Z = (√(Index Variable) − μ)/σ.

Results: There were 692 subjects enrolled in the study. The fitted model equation was offered for each variable with values presented for μ and σ. Modelling with penalized splines was performed for VAT index, IMAT index and total adipose tissue index. Scatterplots of each variable were produced with lines of Z-scores as a visual representation.

Conclusion: This study offers comparative data to allow comparison amongst multiple populations. This will form an important reference for future research and clinical practice.

Keywords

Body composition; Computed tomography; Sarcopenia; Normative data

1. Introduction

In order to progress towards a more personalized approach to patient care, accurate and reproducible biomarkers are required to allow greater accuracy in disease diagnosis, individualize treatment planning and assess outcome response [1]. Body composition is one such biomarker that has demonstrated potential in oncological and surgical settings, such as outcomes following surgery [2,3] and prognosis associated with melanoma, esophageal and colorectal malignancies [4–6]. Markers of skeletal muscle depletion or sarcopenia are also demonstrating potential as a predictor of outcomes in the oncological and surgical setting [7–14]. The association of obesity with societal health problems and resultant healthcare costs is also well established [15–17].

Various techniques have been proposed to allow accurate measurement of body composition, with computed tomography providing a fast, reliable and reproducible method. CT is now widely recognized as a gold standard in the measurement of body composition biomarkers [18–20]. Body composition biomarkers that could be calculated from CT include visceral adipose tissue (VAT) area, subcutaneous adipose tissue (SAT) area, skeletal muscle (SM) area and intermuscular adipose tissue (IMAT) area. Criticisms of multi-slice CT include the use of ionizing radiation and the necessity for labor intensive segmentation [18]. CT is often used in oncological imaging however, and assessment of body composition may be performed on scheduled CT studies. In other scenarios, single slice images have been proposed to decrease effective radiation dose and improve work flow. Single slice images at the level of the umbilicus have been proven to be representative of whole body adipose tissue [21]. Automation and semi-automation of body segmentation will also allow this work to be performed essentially instantaneously [22,23].

Body composition is well recognized to change with age and sex [24]. Normative data is therefore essential to allow adequate comparisons of individuals within a larger population. To the best of our knowledge, prospective population based normative data of body composition measurement in healthy subjects from CT is lacking. The aim of this study is to determine the age and sex specific distribution of body composition data, based on

information gathered from CT. This will serve as a benchmark for further clinical and scientific research.

2. Methods

Ethical approval was attained from the Institutional Review Board with consent waived. This study was compliant with the Health Insurance Portability and Accountability Act. Only patients that consented to the use of medical records for research purposes were included.

2.1. Subjects

This was a prospective study recruiting healthy patients from the medical records linkage of the Rochester Epidemiology Project [25]. All subjects from this cohort were healthy residents of Rochester, Minnesota with the sample age stratified, originally recruited for a bone density study between 1999 and 2001 and inclusion and exclusion criteria are previously described [25,26]. No subject was excluded for our study. The cohort age ranged from 21 to 97 years and was sex-matched per decade, starting from the third. The only exception was in the 6th and 7th decade. Here, females were oversampled to account for the possible effects of hormone replacement therapy. The sample is representative of the population within Rochester, MN, which is predominantly white (98%) with under-representation of the African-American, Asian or Hispanic population.

2.2. CT scan

Each patient had a CT scan without IV contrast (NECT). Scanning was performed on a multi-detector CT scanner (Light Speed QX-I; GE Medical Systems, Wakesha, WI, USA). A tube potential of 120 kVp, tube current of 80 mA, rotation time of 0.8 s, table speed of 7.5 mm/rotation, detector collimation of 4 × 2.5 mm and pitch of 0.75 was used. Standard field of view was 380 mm but this was adjusted up to 500 mm based on patient size. None of the patients had subcutaneous adipose tissue cutoff from the field of view. Images were acquired between T12 to mid L4 vertebral body level, with a slice thickness of 2.5 mm.

2.3. Muscle and adipose tissue quantification

Quantification was performed using previously validated semi-automated in-house developed software for body composition analysis [22]. This software has been previously validated with inter-observer coefficient of variance of 1.5% for subcutaneous adipose tissue area, 1.0% for visceral adipose tissue area and 0.8% for skeletal muscle area. After manually selecting a single axial image at the level of the third lumbar vertebrae (L3) on which both transverse processes were fully observed, the software automatically segmented the image selected and highlighted the segmentation results in three boundaries (Fig. 1) [22]. The program automatically places boundary lines between external air and subcutaneous adipose tissue (boundary 1), between subcutaneous adipose tissue and abdominal wall/paraspinal muscles (boundary 2), and between abdominal wall/paraspinal muscles and visceral adipose tissue (boundary 3). The program also automatically created masks for bone and colon. The reviewer carefully inspected the boundaries with manual correction performed of each boundary if needed. All segmentations were inspected by a radiologist with three years post fellowship experience. Exclusion criteria for CT images include artifact secondary to excess

motion or the presence of metal/barium. Images where the skin surface was not included in the field of view were also excluded.

SAT area was calculated as the area between the boundary 1 and 2 with a CT attenuation value between −190 and −30 HU. The SM area was calculated as area between boundary 2 and boundary 3 with a CT attenuation value between −30 and 150 HU [27]. The IMAT area was calculated as areas between boundary 2 and boundary 3 with a CT attenuation value between −190 and −30 HU [21,28,29]. The VAT area was calculated as areas within boundary 3 with a CT attenuation value between −190 and −30 HU. An index was quantified for measures of body composition by adjusting for subject height in metres^2.

2.4. Statistical analyses

Generalized Additive Models for Location, Scale and Shape (GAMLSS) were used to assess the location, scale, and shape of each variable across age, stratified by sex. Models were fit using the gamlss function from the gamlss R package (version 5.1.5) and run using R (version 3.6.2). For each variable (or square root of the variable), models were fit describing the μ (mean) and σ (standard deviation) as follows: $\mu = a_0 + a_1 \times age^{1.5}$ and $\log(\sigma) = b_0 + b_1 \times age^{1.5}$. If the relationship between age and μ or σ was not linear, penalized splines were instead used in the formulas.

Z-scores specific to sex were assessed for each of the parameters analyzed: VAT index, SAT index, SM index, IMAT index, and total adipose tissue (TAT) index. Age-specific z-scores were calculated using the formula:

$$Z = (\text{Index Variable} - \mu)/\sigma \text{ or } Z = (\sqrt{}(\text{Index Variable}) - \mu)/\sigma$$

Spearman correlation coefficient was utilized to compare body mass index (BMI) to measures of body composition. BMI grading was based on the World Health Organization classification [30].

3. Results

3.1. Demographics

There were 692 subjects enrolled in the study, 374 female and 318 male. Age ranged from 21 to 97 years. There were 25 male and 25 female subjects aged 20–29, randomly sampled from the cohort. Following this, 50 subjects from each sex were sampled for each decade to the 8th decade, except for females in their 6th and 7th decade where 25 extra subjects in each decade were sampled (therefore 75 subjects in the female group and 50 in the male group in these age groups). In the final category of 80 years and older there were 45 females aged 80–89 years with 4 subjects aged over 90 years. There were 39 males aged 80–89 years with 4 subjects aged over 90 years.

The body mass index (BMI) of the cohort based on sex and age is outlined in Table 1. Overall there were four subjects classified as underweight (1%; Female 1%; Male 0%), 195 subjects of normal weight (28%, F35%, M20%), 284 subjects classified as overweight (41%; F35%; M48%) and 209 subjects classified as obese (30%; F29%; M32%). With

respect to ethnicity, 99% of the female population was white with 96% of the male sample. The correlation of BMI to measures of indexed body composition is outlined in Table 2. The strongest correlation is to indexed total adipose tissue area and indexed subcutaneous adipose tissue area with poor correlation to skeletal muscle index.

3.2. Skeletal muscle (SM) index

Scatter plot of SM index with lines for z-score is demonstrated in Fig. 2. The fitted model for SM Index is given as follows: SM Index ~ Normal(μ, σ), where μ = 43.88 + −0.01003 $age^{1.5}$, and log(σ) = 1.651 (female) and μ = 60.16 + −0.02070 $age^{1.5}$ and log(σ) = 2.012 + 0.0003535 $age^{1.5}$ (male). Z value can be calculated using the following formula: $z = (SM\ Index - \mu)/\sigma$.

Mean SM index reveals a progressive decline in both male and female subjects from the beginning of the third decade. This is more pronounced in male patients. Based on the assessment of residuals, variability is similar between both sexes.

3.3. Subcutaneous adipose tissue (SAT) index

Scatter plot of SAT index with lines for z-score is demonstrated in Fig. 3. The fitted model for SAT index is given as follows: √(SAT index) ~ Normal(μ, σ), where μ = 8.276 + 0.0003651 $age^{1.5}$, and log(σ) = 1.084 + −0.0005786 $age^{1.5}$ (female) and μ = 7.359 + 0.0002681 $age^{1.5}$ and log(σ) = 0.8327 + −0.0009524 $age^{1.5}$ (male). Z value can be calculated using the following formula: $z = (\sqrt{(SAT\ index)} - \mu)/\sigma$.

SAT index remains relatively stable for male subjects throughout adult life. In female subjects there is a gradual increase in SAT index to the 7th and 8th decade with a decline into the 9th decade. There is increased variability in the female population which persists following a transformation.

3.4. Visceral adipose tissue (VAT) index

Scatter plot VAT index with lines for z-score is demonstrated in Fig. 4. The fitted model for VAT index is given as follows: √(VAT index) ~ Normal(μ, σ), where the relationship of age with μ and σ was modeled using penalized splines. The values for μ and σ are both are shown in Table 3. *Z value can be calculated using the following formula:* $z = (\sqrt{(VAT\ index)}\ \hat{R}\ \mu)/\sigma$.

Mean VAT index is increased in males versus females. Levels increase in both males and females from the 3rd to the 7th decade, plateauing over the 8th decade.

3.5. Intermuscular adipose tissue (IMAT) index

Scatter plot of IMAT index with lines for z-score is demonstrated in Fig. 5. The fitted model for IMAT index is given as follows: √(IMAT index) ~ Normal(μ, σ), where the relationship of age with μ and σ was modeled using penalized splines. The values for μ and σ are both are shown in Table 4. *Z value can be calculated using the following formula:* $z = (\sqrt{(IMAT\ index)}\ \hat{R}\ \mu)/\sigma$.

Mean IMAT index is similar for males and females throughout the age range of the cohort. There is a progressive increase in mean IMAT index from the 3rd to 9th decade. This correlates negatively with skeletal muscle volume, in that as intramuscular adipose tissue increases, skeletal volume decreases. Variability in IMAT index was similar for males and females.

3.6. Total adipose tissue (TAT) index

Scatter plot of TAT index with lines for z-score is demonstrated in Fig. 6. The fitted model for TAT index is given as follows: $\sqrt{}$(TAT index) ~ Normal(μ, σ), where the relationship of age with μ and σ was modeled using penalized splines. The values for μ and σ are both are shown in Table 5. *Z value can be calculated using the following formula:* $z = (\sqrt{}(\text{TAT index}) - \mu)/\sigma$.

Mean TAT index is similar for both males and females. There is a progressive increase in values from the 3rd to the 7th decade with then a plateau onwards.

4. Discussion

This study offers normative data derived from a population-specific cohort of North Americans for multiple measured of body composition, potentially allowing comparisons to the general population. The results demonstrate that these measures of body composition are variable depending on age and sex.

This study demonstrates that skeletal muscle volume, as measured by SM index, decreases with age. Sarcopenia is well recognized adverse effect of aging [31–33]. SM index, defined as the area of muscular tissue, divided by the patient height (squared), is widely accepted as a surrogate for a measure of sarcopenia [34,35]. The utility of CT as a measure of muscle mass is regarded as gold standard with the usage of a single slice through the level of the lumbar vertebrae as an accurate predictor of muscle area throughout the whole body [34,36–38]. This paper also demonstrates that IMAT index increases with age, coinciding with decreasing muscle area. Unlike adipose tissue in other body compartments, this increase continues nearing end-of-life. Our findings correlate to the results of other studies [39–42]. Sarcopenia is a quantitative and qualitative decline in muscle function. In the elderly population, even in the absence of disease, loss of strength far outweighs muscle volume loss [43–46]. The increase of intermuscular adipose tissue is postulated as partially responsible for this imbalance secondary to the lipotoxic effects on the muscle [41,47,48].

Variations in adipose tissue deposition have been associated with the development of multiple morbidities and are dependent on factors such as age and sex [49]. There are four major compartments of adipose tissue deposition: subcutaneous, visceral, bone marrow and perivascular. Adipose tissue within these compartments all demonstrate different functions, from the storage of energy in the visceral compartment [50], to the provision of insulation and cushioning in the subcutaneous compartment [51]. As a result, the volume within each compartment varies throughout adult life.

Mean SAT index demonstrated variations in our study based on age and sex. SAT index remained relatively stable in the male subjects. Female patients demonstrated a rise in SAT index until the 5th or 6th decade with a decline until end of life. VAT index of the population in our cohort was higher in male subjects, with values in both sexes increasing by age until the 7th/8th decade with subsequent decline. The age and sex related changes in VAT index and SAT index are similar to other studies [52–55].

The reason behind the shift in body adipose tissue distribution based on age and sex is unclear, with theories of alcohol consumption and hormonal changes as contributing factors [56–58]. Estrogens in particular are believed to play a significant role in premenopausal women promoting adipose tissue deposition in the glutofemoral region [59]. In postmenopausal females, the shift changes to increased visceral adipose tissue [55,60]. It has been demonstrated however, that hormone replacement therapy maintains premenopausal adipose tissue deposition, strengthening the role of estrogens in this process [61]. VAT is independently associated with the development of multiple metabolic and neoplastic conditions [4–6,62,63]. Conventional measures of adiposity however may be insufficient to assess for the variations in body adipose tissue distribution. For instance, total body weight gain does not correlate accurately to VAT increase [57,64]. Also, as apparent in this study, BMI correlates with total body adipose tissue and subcutaneous adipose tissue but is a poor reflection for changes in skeletal muscle index. This is why multi-compartmental measures of body composition are required.

There is an abundance of methods to measure body composition. Traditional measures such as skinfold thickness, BMI or waist circumference; predictive techniques such as bioelectric impedance analysis; and finally multi-component techniques such as dual energy x-ray absorptiometry, MRI/CT and hydrometry [65]. The provision of normative data from many of these methods however, is lacking. This is the first study offering normative data using cross-sectional, multi-compartmental assessment of body composition.

The creation of a z-score allows the comparison of a dependent variable between groups when there are continuous independent variables. It allows a comparison of values from two different populations, given a normal distribution. In order to create a z-score, regression analysis of the mean and standard deviation of the normal population is required. Its utility is demonstrated in multiple clinical settings, from infant growth curves to bone mineral density calculations.

There are a number of limitations to this study. The retrospective nature obviously introduces a certain quantity of selection bias. The population also only consists of subjects from Olmsted County in Minnesota. This cohort is predominantly white from European ancestry and may not reflect the black or Asian population. In this study, CT scans were obtained without intravenous contrast and using very low radiation dose, while most of clinical CT scans are obtained with intravenous contrast. The attenuation values of muscle and adipose tissue are known to increase with intravenous contrast, but increase in the SM area and decrease SAT, VAT and IMAT area is probably small [66–69]. There is also decreased numbers at the upper extremities of age in the cohort (>90), meaning interpretation of data in this age-group should be performed with caution. In terms of the

statistical method, the use of the GAMLSS approach is that in the literature generally these models are fit with larger sample sizes, greater than 1000 subjects. As the numbers for this study are relatively small, the utility of this model may not be ideal.

In conclusion, this study describes trends in measures of body composition, describing multi-compartmental variations depending on age and sex. This study offers comparative data to allow comparison amongst multiple populations and forms an important reference for future research and clinical practice.

Grant support

This work was supported by NIH grants AR027065 and UL1 TR002377 (Mayo Clinic CTSA).

References

[1]. Scharf G, Heineke J. Finding good biomarkers for sarcopenia. J Cachexia Sarcopenia Muscle 2012;3(3):145–8. [PubMed: 22911244]

[2]. Saitoh-Maeda Y, Kawahara T, Miyoshi Y, Tsutsumi S, Takamoto D, Shimokihara K, et al. A low psoas muscle volume correlates with a longer hospitalization after radical cystectomy. BMC urol 2017;17(1):87. [PubMed: 28923108]

[3]. Englesbe MJ, Lee JS, He K, Fan L, Schaubel DE, Sheetz KH, et al. Analytic morphomics, core muscle size, and surgical outcomes. Annal surg 2012;256(2):255–61.

[4]. Saeed N, Shridhar R, Almhanna K, Hoffe S, Chuong M, Meredith K. CT-based assessment of visceral adiposity and outcomes for esophageal adenocarcinoma. J Gastrointest Oncol 2017;8(5):833–41. [PubMed: 29184687]

[5]. Grignol VP, Smith AD, Shlapak D, Zhang X, Del Campo SM, Carson WE. Increased visceral to subcutaneous fat ratio is associated with decreased overall survival in patients with metastatic melanoma receiving anti-angiogenic therapy. Surg Oncol 2015;24(4):353–8. [PubMed: 26690825]

[6]. Rickles AS, Iannuzzi JC, Mironov O, Deeb AP, Sharma A, Fleming FJ, et al. Visceral obesity and colorectal cancer: are we missing the boat with BMI? J Gastrointest Surg 2013;17(1):133–43. discussion p.43. [PubMed: 23090279]

[7]. Lee JS, He K, Harbaugh CM, Schaubel DE, Sonnenday CJ, Wang SC, et al. Frailty, core muscle size, and mortality in patients undergoing open abdominal aortic aneurysm repair. J Vasc Surg 2011;53(4):912–7. [PubMed: 21215580]

[8]. Moisey LL1 MM, Cotton BA, Premji T, Heyland DK, Wade CE, Bulger E, Kozar RA, for the Nutrition and Rehabilitation Investigators Consortium (NUTRIC). Skeletal muscle predicts ventilator-free days, ICU-free days, and mortality in elderly ICU patients. Crit Care Sep 19 2013;17(5):R206 [Epub ahead of print]. [PubMed: 24050662]

[9]. Kasahara R, Kawahara T, Ohtake S, Saitoh Y, Tsutsumi S, Teranishi JI, et al. A low psoas muscle index before treatment can predict a poorer prognosis in advanced bladder cancer patients who receive gemcitabine and nedaplatin therapy. Biomed Res Int 2017;2017:7981549. [PubMed: 28497065]

[10]. Deng CY, Lin YC, Wu JS, Cheung YC, Fan CW, Yeh KY, et al. Progressive sarcopenia in patients with colorectal cancer predicts survival. AJR Am J Roentgenol 2018;210(3):526–32. [PubMed: 29364725]

[11]. Psutka SP, Carrasco A, Schmit GD, Moynagh MR, Boorjian SA, Frank I, et al. Sarcopenia in patients with bladder cancer undergoing radical cystectomy: impact on cancer-specific and all-cause mortality. Cancer 2014;120(18): 2910–8. [PubMed: 24840856]

[12]. Lee JS, Kim YS, Kim EY, Jin W. Prognostic significance of CT-determined sarcopenia in patients with advanced gastric cancer. PloS One 2018;13(8): e0202700. [PubMed: 30125312]

[13]. Prado CM. Prevalence and clinical implications of sarcopenic obesity in patients with solid tumors of the respiratory and gastrointestinal tracts: a population-based study. Lancet Oncol 2008 Jul;9(7):629–35. 10.1016/S1470-2045(08)70153-0. Epub 2008 Jun 6. [PubMed: 18539529]

[14]. Zamboni M Sarcopenic obesity: a new category of obesity in the elderly. Nutr Metab Cardiovasc Dis 2008 Jun;18(5):388–95. 10.1016/jnumecd200710002. Epub 2008 Apr 18. [PubMed: 18395429]

[15]. Afshin A, Forouzanfar MH, Reitsma MB, Sur P, Estep K, Lee A, et al. Health Effects of Overweight and Obesity in 195 Countries over 25 Years. New Engl J Med 2017;377(1):13–27. [PubMed: 28604169]

[16]. Cawley J, Meyerhoefer C. The medical care costs of obesity: an instrumental variables approach. J Health Econ 2012;31(1):219–30. [PubMed: 22094013]

[17]. Finkelstein EA, Trogdon JG, Cohen JW, Dietz W. Annual medical spending attributable to obesity: payer-and service-specific estimates. Health Aff (Project Hope) 2009;28(5):w822–31.

[18]. Borga M, West J, Bell JD, Harvey NC, Romu T, Heymsfield SB, et al. Advanced body composition assessment: from body mass index to body composition profiling. J Investig Med 2018;66(5):1–9.

[19]. Cesari M, Fielding RA, Pahor M, Goodpaster B, Hellerstein M, van Kan GA, et al. Biomarkers of sarcopenia in clinical trials-recommendations from the International Working Group on Sarcopenia. J Cachexia Sarcopenia Muscle 2012;3(3):181–90. [PubMed: 22865205]

[20]. Muller MJ, Braun W, Pourhassan M, Geisler C, Bosy-Westphal A. Application of standards and models in body composition analysis. Proc Nutr Soc 2016;75(2):181–7. [PubMed: 26541411]

[21]. Yoshizumi T, Nakamura T, Yamane M, Islam AH, Menju M, Yamasaki K, et al. Abdominal fat: standardized technique for measurement at CT. Radiology 1999;211(1):283–6. [PubMed: 10189485]

[22]. Takahashi N, Sugimoto M, Psutka SP, Chen B, Moynagh MR, Carter RE. Validation study of a new semi-automated software program for CT body composition analysis. Abdom Radio 2017;42(9):2369–75.

[23]. Weston AD, Korfiatis P, Kline TL, Philbrick KA, Kostandy P, Sakinis T, et al. Automated abdominal segmentation of CT scans for body composition analysis using deep learning. Radiology 2019;290(3):669–79. [PubMed: 30526356]

[24]. St-Onge MP, Gallagher D. Body composition changes with aging: the cause or the result of alterations in metabolic rate and macronutrient oxidation? Nutrition 2010;26(2):152–5. [PubMed: 20004080]

[25]. Melton LJ 3rd. History of the Rochester epidemiology project. Mayo Clinic Proceed 1996;71(3):266–74.

[26]. Khosla S, Riggs BL, Atkinson EJ, Oberg AL, McDaniel LJ, Holets M, et al. Effects of sex and age on bone microstructure at the ultradistal radius: a population-based noninvasive in vivo assessment. J Bone Miner Res. 2006;21(1):124–31. [PubMed: 16355281]

[27]. Aubrey J, Esfandiari N, Baracos VE, Buteau FA, Frenette J, Putman CT, et al. Measurement of skeletal muscle radiation attenuation and basis of its biological variation. Acta Physiol (Oxf) 2014;210(3):489–97. [PubMed: 24393306]

[28]. Sjostrom L, Kvist H, Cederblad A, Tylen U. Determination of total adipose tissue and body fat in women by computed tomography, 40K, and tritium. Am J Physiol 1986;250(6 Pt 1):E736–45. [PubMed: 3717334]

[29]. Kvist H, Chowdhury B, Sjostrom L, Tylen U, Cederblad A. Adipose tissue volume determination in males by computed tomography and 40K. Int J Obes 1988;12(3):249–66. [PubMed: 3391740]

[30]. Organization WH. Obesity: preventing and managing the global epidemic. Report of a WHO consultation. World Health Organ Tech Rep Ser 2000;894(ixii):1–253.

[31]. Larsson L, Degens H, Li M, Salviati L, Lee YI, Thompson W, et al. Sarcopenia: aging-related loss of muscle mass and function. Physiol Rev 2019;99(1): 427–511. [PubMed: 30427277]

[32]. Jackson AS, Janssen I, Sui X, Church TS, Blair SN. Longitudinal changes in body composition associated with healthy ageing: men, aged 20–96 years. Br J Nutr 2012;107(7):1085–91. [PubMed: 21810289]

[33]. He X, Li Z, Tang X, Zhang L, Wang L, He Y, et al. Age- and sex-related differences in body composition in healthy subjects aged 18 to 82 years. Medicine (Baltimore) 2018;97(25):e11152. [PubMed: 29924020]

[34]. Fearon K, Strasser F, Anker SD, Bosaeus I, Bruera E, Fainsinger RL, et al. Definition and classification of cancer cachexia: an international consensus. Lancet Oncol 2011;12(5):489–95. [PubMed: 21296615]

[35]. Golse N, Bucur PO, Ciacio O, Pittau G, Sa Cunha A, Adam R, et al. A new definition of sarcopenia in patients with cirrhosis undergoing liver transplantation. Liver Transpl 2017;23(2):143–54. [PubMed: 28061014]

[36]. Mourtzakis M, Prado CM, Lieffers JR, Reiman T, McCargar LJ, Baracos VE. A practical and precise approach to quantification of body composition in cancer patients using computed tomography images acquired during routine care. Appl Physiol Nutr Metab 2008;33(5):997–1006. [PubMed: 18923576]

[37]. Montano-Loza AJ, Meza-Junco J, Baracos VE, Prado CM, Ma M, Meeberg G, et al. Severe muscle depletion predicts postoperative length of stay but is not associated with survival after liver transplantation. Liver Transpl 2014;20(6): 640–8. [PubMed: 24678005]

[38]. Shen W, Punyanitya M, Wang Z, Gallagher D, St-Onge MP, Albu J, et al. Total body skeletal muscle and adipose tissue volumes: estimation from a single abdominal cross-sectional image. J Appl Physiol (1985) 2004;97(6):2333–8. [PubMed: 15310748]

[39]. Cree MG, Newcomer BR, Katsanos CS, Sheffield-Moore M, Chinkes D, Aarsland A, et al. Intramuscular and liver triglycerides are increased in the elderly. J Clin Endocrinol Metab 2004;89(8):3864–71. [PubMed: 15292319]

[40]. Gallagher D, Kuznia P, Heshka S, Albu J, Heymsfield SB, Goodpaster B, et al. Adipose tissue in muscle: a novel depot similar in size to visceral adipose tissue. Am J Clin Nutr 2005;81(4):903–10. [PubMed: 15817870]

[41]. Goodpaster BH, Carlson CL, Visser M, Kelley DE, Scherzinger A, Harris TB, et al. Attenuation of skeletal muscle and strength in the elderly: The Health ABC Study. J Appl Physiol (1985) 2001;90(6):2157–65. [PubMed: 11356778]

[42]. Nakagawa Y, Hattori M, Harada K, Shirase R, Bando M, Okano G. Age-related changes in intramyocellular lipid in humans by in vivo H-MR spectroscopy. Gerontology 2007;53(4):218–23. [PubMed: 17356288]

[43]. Evans WJ, Cyr-Campbell D. Nutrition, exercise, and healthy aging. J Am Diet Assoc. 1997;97(6):632–8. [PubMed: 9183325]

[44]. Vandervoort AA. Aging of the human neuromuscular system. Muscle Nerve 2002;25(1):17–25. [PubMed: 11754180]

[45]. Frontera WR, Hughes VA, Fielding RA, Fiatarone MA, Evans WJ, Roubenoff R. Aging of skeletal muscle: a 12-yr longitudinal study. J Appl Physiol (1985) 2000;88(4):1321–6. [PubMed: 10749826]

[46]. Goodpaster BH, Park SW, Harris TB, Kritchevsky SB, Nevitt M, Schwartz AV, et al. The loss of skeletal muscle strength, mass, and quality in older adults: the health, aging and body composition study. J Gerontol A Biol Sci Med Sci. 2006;61(10):1059–64. [PubMed: 17077199]

[47]. Clark BC, Manini TM. Sarcopenia =/= dynapenia. J Gerontol A Biol Sci Med Sci. 2008;63(8):829–34. [PubMed: 18772470]

[48]. Visser M, Kritchevsky SB, Goodpaster BH, Newman AB, Nevitt M, Stamm E, et al. Leg muscle mass and composition in relation to lower extremity performance in men and women aged 70 to 79: the health, aging and body composition study. J Am Geriatr Soc. 2002;50(5):897–904. [PubMed: 12028178]

[49]. Mancuso P, Bouchard B. The impact of aging on adipose function and adipokine synthesis. Front Endocrinol (Lausanne) 2019;10:137. [PubMed: 30915034]

[50]. Goossens GH. The role of adipose tissue dysfunction in the pathogenesis of obesity-related insulin resistance. Physiol Behav 2008;94(2):206–18. [PubMed: 18037457]

[51]. Karpe F, Pinnick KE. Biology of upper-body and lower-body adipose tissue–link to whole-body phenotypes. Nat Rev Endocrinol 2015;11(2):90–100. [PubMed: 25365922]

[52]. Swainson MG, Batterham AM, Hind K. Age- and sex-specific reference intervals for visceral fat mass in adults. Int J Obes 2019.

[53]. Hunter G, Lara-Castro C, Byrne N, Zakharkin S, StOnge M, Allison D. Weight loss needed to maintain visceral adipose tissue during aging. Int J Body Compos Res 2005;3(2):55.

[54]. Miazgowski T, Kucharski R, Soltysiak M, Taszarek A, Miazgowski B, Widecka K. Visceral fat reference values derived from healthy European men and women aged 20–30 years using GE Healthcare dual-energy x-ray absorptiometry. PloS one 2017;12(7):e0180614. [PubMed: 28683146]

[55]. Lee CG, Carr MC, Murdoch SJ, Mitchell E, Woods NF, Wener MH, et al. Adipokines, inflammation, and visceral adiposity across the menopausal transition: a prospective study. J Clin Endocrinol Metab 2009;94(4):1104–10. [PubMed: 19126626]

[56]. Larson DE, Hunter GR, Williams MJ, Kekes-Szabo T, Nyikos I, Goran MI. Dietary fat in relation to body fat and intraabdominal adipose tissue: a cross-sectional analysis. Am J Clin Nutr 1996;64(5):677–84. [PubMed: 8901785]

[57]. Hunter GR, Gower BA, Kane BL. Age related shift in visceral fat. Int J Body Compos Res. 2010;8(3):103–8. [PubMed: 24834015]

[58]. Frank AP, de Souza Santos R, Palmer BF, Clegg DJ. Determinants of body fat distribution in humans may provide insight about obesity-related health risks. J Lipid Res. 2019;60(10):1710–9. [PubMed: 30097511]

[59]. Wells JC. Sexual dimorphism of body composition. Best Pract Res Clinical Endocrinol Metabol 2007;21(3):415–30.

[60]. Abdulnour J, Doucet E, Brochu M, Lavoie JM, Strychar I, Rabasa-Lhoret R, et al. The effect of the menopausal transition on body composition and cardiometabolic risk factors: a Montreal-Ottawa New Emerging Team group study. Menopause 2012;19(7):760–7. [PubMed: 22395454]

[61]. Papadakis GE, Hans D, Rodriguez EG, Vollenweider P, Waeber G, Marques-Vidal P, et al. Menopausal hormone therapy is associated with reduced total and visceral adiposity: the OsteoLaus cohort. J Clin Endocrinol Metabol 2018;103(5):1948–57.

[62]. Bjorntorp P Classification of obese patients and complications related to the distribution of surplus fat. Nutrition 1990;6(2):131–7. [PubMed: 2134524]

[63]. Filipovsky J, Ducimetiere P, Darne B, Richard JL. Abdominal body mass distribution and elevated blood pressure are associated with increased risk of death from cardiovascular diseases and cancer in middle-aged men. The results of a 15- to 20-year follow-up in the Paris prospective study I. Int J Obes Relat Metab Disord 1993;17(4):197–203. [PubMed: 8387968]

[64]. Thomas GN, Ho SY, Lam KS, Janus ED, Hedley AJ, Lam TH. Impact of obesity and body fat distribution on cardiovascular risk factors in Hong Kong Chinese. Obes Res 2004;12(11):1805–13. [PubMed: 15601976]

[65]. Wells JCK, Fewtrell MS. Measuring body composition. Arch Dis Child 2006;91(7):612–7. [PubMed: 16790722]

[66]. Boutin RD, Kaptuch JM, Bateni CP, Chalfant JS, Yao L. Influence of IV contrast administration on CT measures of muscle and bone attenuation: implications for sarcopenia and osteoporosis evaluation. AJR Am J Roentgenol 2016;207(5): 1046–54. [PubMed: 27556335]

[67]. van der Werf A, Dekker IM, Meijerink MR, Wierdsma NJ, de van der Schueren MAE, Langius JAE. Skeletal muscle analyses: agreement between non-contrast and contrast CT scan measurements of skeletal muscle area and mean muscle attenuation. Clin Physiol Funct Imag 2018;38(3):366–72.

[68]. Morsbach F, Zhang YH, Martin L, Lindqvist C, Brismar T. Body composition evaluation with computed tomography: contrast media and slice thickness cause methodological errors. Nutrition 2019;59:50–5. [PubMed: 30419500]

[69]. Rollins KE, Javanmard-Emamghissi H, Awwad A, Macdonald IA, Fearon KCH, Lobo DN. Body composition measurement using computed tomography: Does the phase of the scan matter? Nutrition 2017;41:37–44. [PubMed: 28760426]

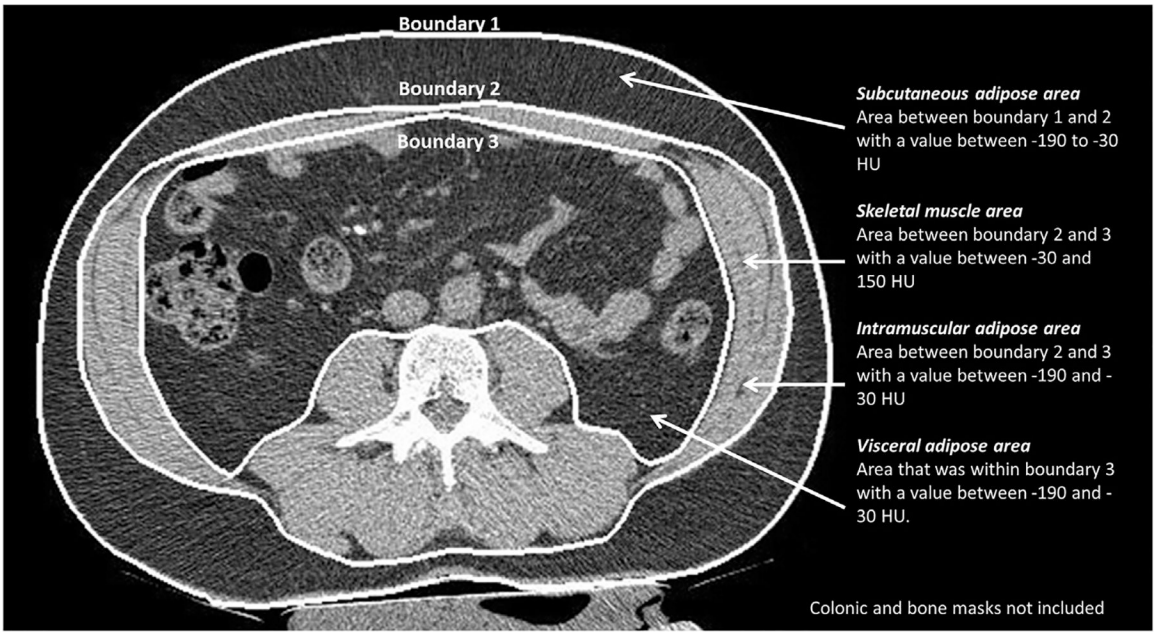

Fig. 1. Method of automated segmentation on a 2.5 mm slice through L3 vertebral body.
The program automatically places three boundary lines. Bone and colonic masks were automatically created by the software to prevent their inclusion in the calculation of measures of body composition.

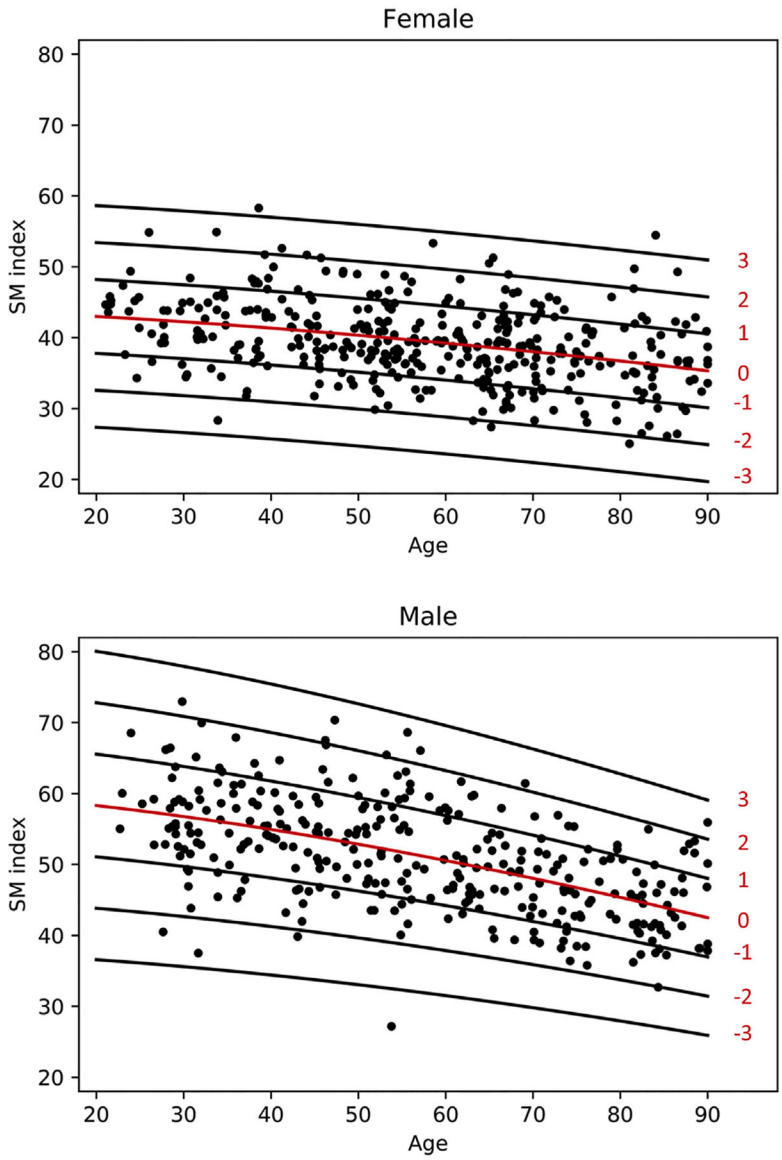

Fig. 2.
Scatterplot of SM Index for females and males with lines of Z-scores.

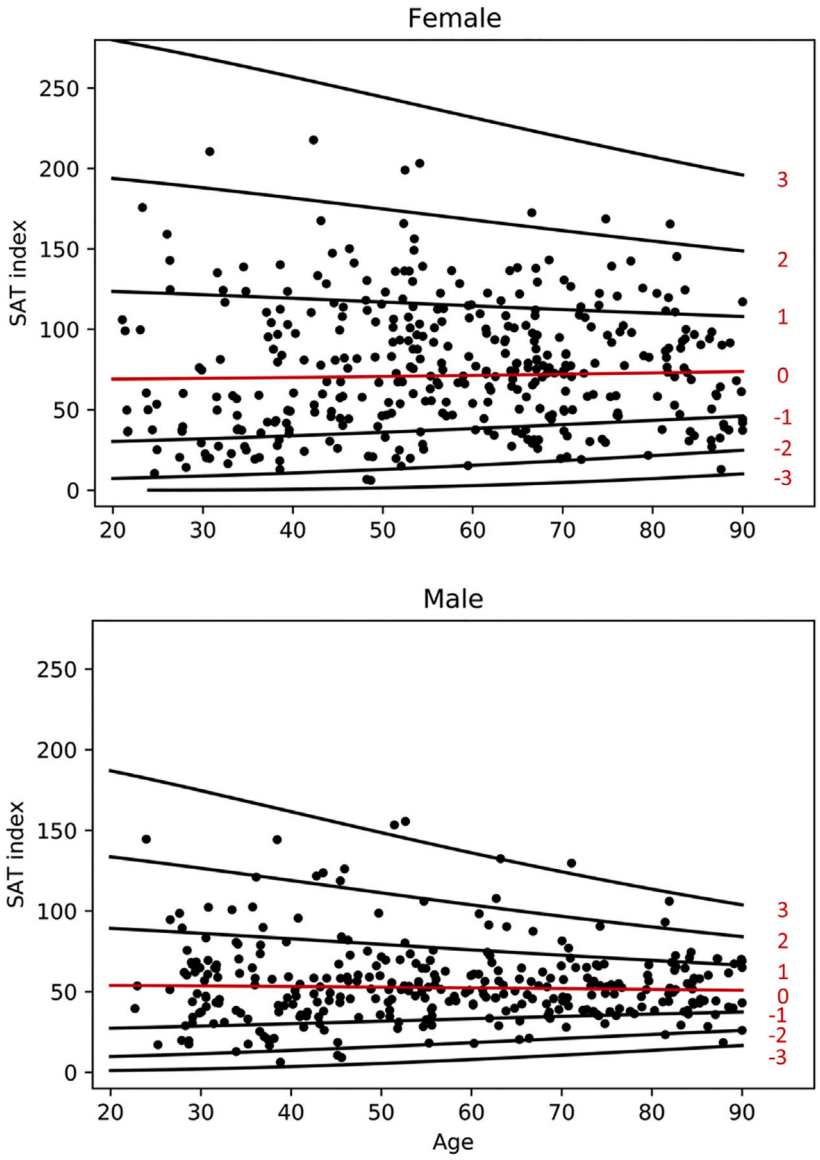

Fig. 3.
Scatterplot of SAT Index for females and males with lines of Z-scores.

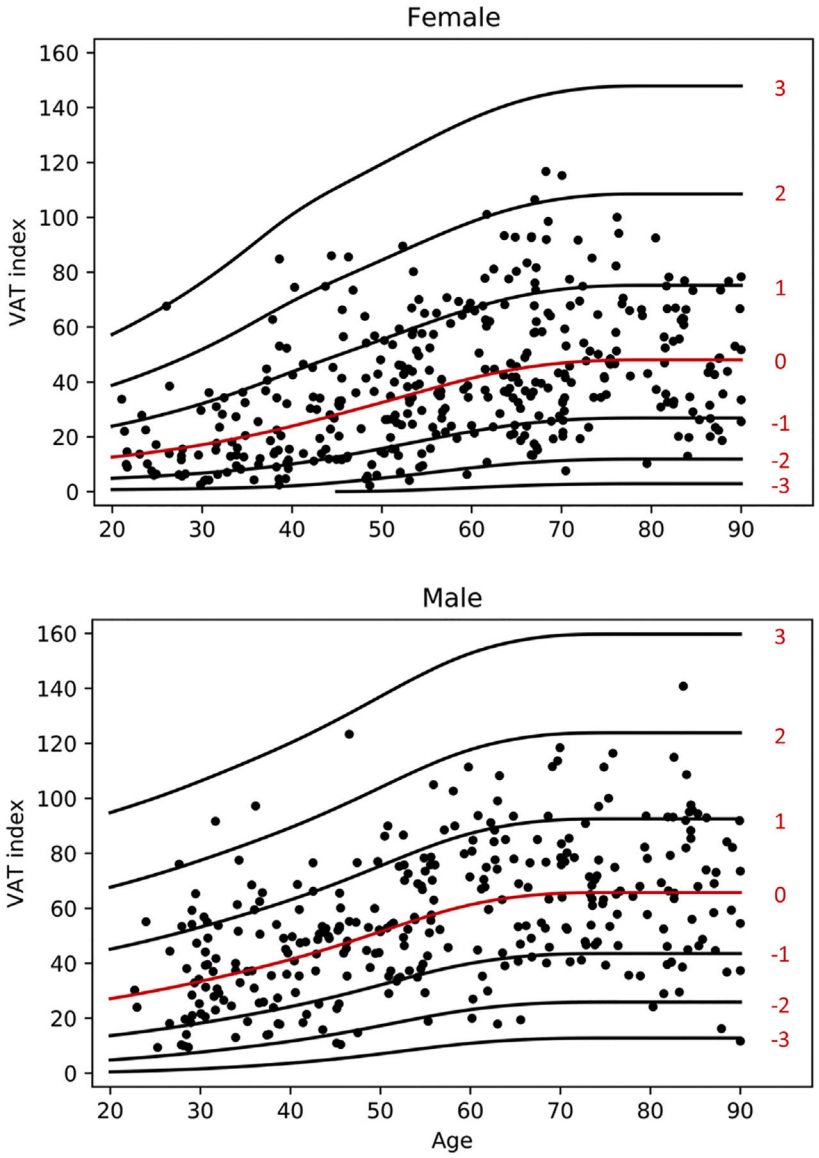

Fig. 4.
Scatterplot of VAT Index for females and males with lines of Z-scores.

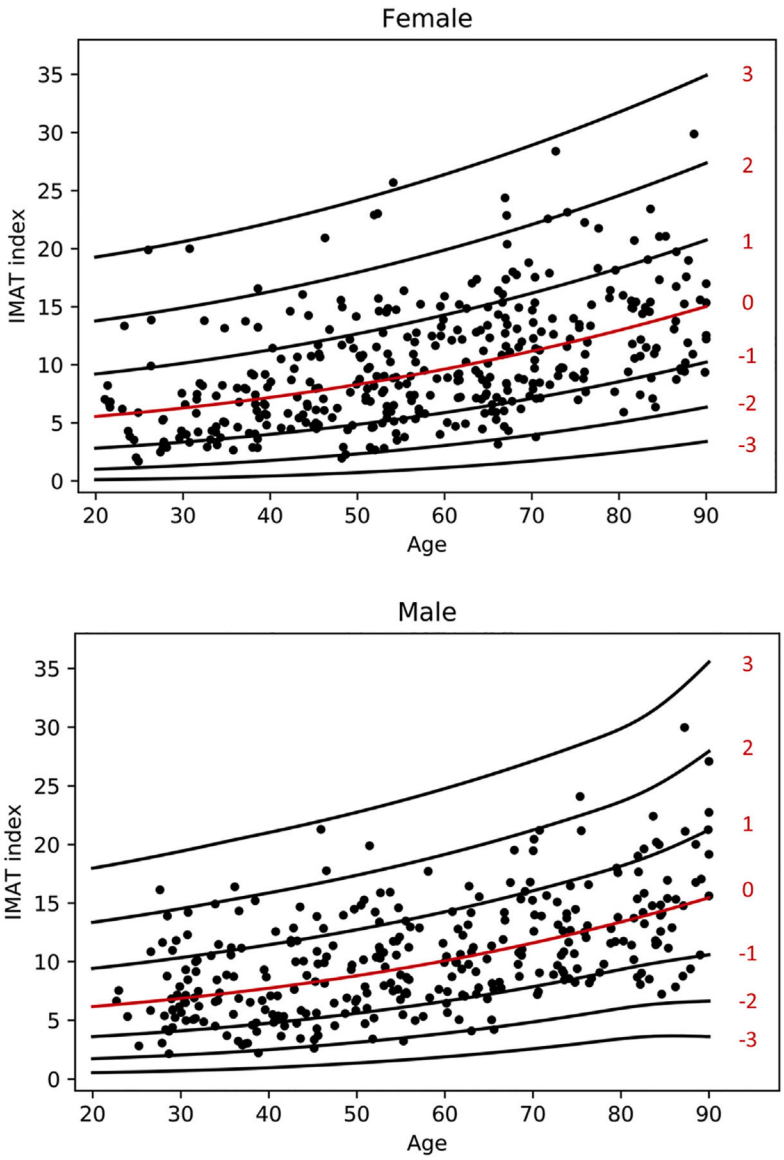

Fig. 5.
Scatterplot of IMAT Index for females and males with lines of Z-scores.

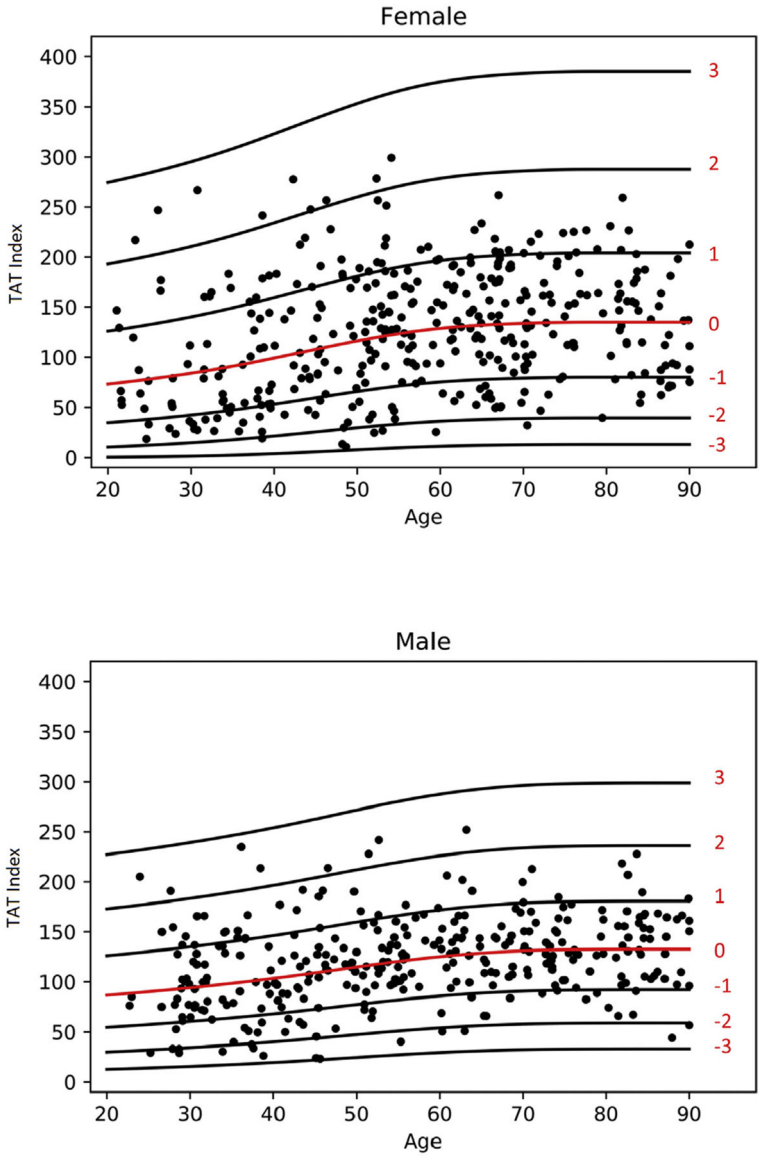

Fig. 6.
Scatterplot of TAT Index for females and males with lines of Z-scores.

Table 1

Body mass index of the cohort based on the WHO criteria for males and females in various age groups.

BMI		20–49 years	50–69 years	70–98 years
Female				
16–18.49	Underweight	1	1	2
18.5–24.9	Normal weight	63	37	31
25–29.9	Overweight	29	61	41
30–34.9	Obese I	18	30	19
35–39.9	Obese II	6	10	6
40–59.9	Obese III	8	11	0
Total		**125**	**150**	**99**
Male				
16–18.49	Underweight	0	0	0
18.5–24.9	Normal weight	31	15	18
25–29.9	Overweight	50	47	56
30–34.9	Obese I	32	30	15
35–39.9	Obese II	8	6	3
40–59.9	bese III	4	2	1
Total		**125**	**100**	**93**

Table 2

Spearman correlation coefficients of BMI and indexed measures of body composition.

	Female		Male	
	Spearman correlation coefficients	**P value**	**Spearman correlation coefficients**	**P value**
SM Index	0.26	<0.001	0.19	0.001
IMAT index	0.61	<0.001	0.59	<0.001
SAT index	0.87	<0.001	0.74	<0.001
VAT index	0.72	<0.001	0.53	<0.001
Total Adipose Tissue index	0.89	<0.001	0.77	<0.001

Clin Nutr. Author manuscript; available in PMC 2022 June 22.

Table 3

Values of mu and sigma for VAT Index based on age and sex.

Age	Female mu	Female sigma	Male mu	Male sigma
20–24	3.6514	1.3781	5.3097	1.5107
25–29	3.9392	1.4748	5.5941	1.5107
30–34	4.2699	1.5761	5.9029	1.5107
35–39	4.6469	1.6747	6.2269	1.5107
40–44	5.0529	1.7327	6.5706	1.5107
45–49	5.4607	1.7430	6.9423	1.5107
50–54	5.8575	1.7431	7.3228	1.5107
55–59	6.2292	1.7431	7.6625	1.5107
60–64	6.5401	1.7431	7.9066	1.5107
65–69	6.7576	1.7431	8.0453	1.5107
70–74	6.8810	1.7431	8.1001	1.5107
75–79	6.9265	1.7431	8.1072	1.5107
80–84	6.9302	1.7431	8.1072	1.5107
85–89	6.9302	1.7431	8.1072	1.5107

Table 4

Values of mu and sigma for IMAT Index based on age and sex.

Age	Female mu	Female sigma	Male mu	Male sigma
20–24	2.3834	0.6780	2.5100	0.5870
25–29	2.4571	0.6780	2.5773	0.5922
30–34	2.5380	0.6780	2.6513	0.5986
35–39	2.6256	0.6780	2.7314	0.6001
40–44	2.7193	0.6780	2.8174	0.6006
45–49	2.8187	0.6780	2.9092	0.6006
50–54	2.9236	0.6780	3.0068	0.6006
55–59	3.0337	0.6780	3.1099	0.6006
60–64	3.1487	0.6780	3.2188	0.6006
65–69	3.2684	0.6780	3.3337	0.6006
70–74	3.3927	0.6780	3.4543	0.6006
75–79	3.5214	0.6780	3.5802	0.6007
80–84	3.6543	0.6780	3.7113	0.6091
85–89	3.8053	0.6780	3.8613	0.6503

Table 5

Values of mu and sigma for Total Adipose Tissue Index based on age and sex.

Age	Female mu	Female sigma	Male mu	Male sigma
20–24	8.6695	2.6700	9.3816	1.9212
25–29	8.9703	2.6700	9.5749	1.9212
30–34	9.3138	2.6700	9.7879	1.9212
35–39	9.7057	2.6700	10.0206	1.9212
40–44	10.1302	2.6700	10.2761	1.9212
45–49	10.5476	2.6700	10.5507	1.9212
50–54	10.9217	2.6700	10.8227	1.9212
55–59	11.2161	2.6700	11.0644	1.9212
60–64	11.4117	2.6700	11.2561	1.9212
65–69	11.5248	2.6700	11.3902	1.9212
70–74	11.5874	2.6700	11.4699	1.9212
75–79	11.6147	2.6700	11.5050	1.9212
80–84	11.6172	2.6700	11.5177	1.9212
85–89	11.6172	2.6700	11.5204	1.9212